

## Physical and Kinetic Analysis of the Cooperative Role of Metal Ions in Catalysis of Phosphodiester Cleavage by a Dinuclear Zn(II) Complex

Olga Iranzo, Andrey Y. Kovalevsky, Janet R. Morrow,\* and John P. Richard\*

Contribution from the Department of Chemistry, University at Buffalo, The State University of New York, Buffalo, New York 14260-3000

Received July 16, 2002; E-mail: jrRichard@chem.buffalo.edu

**Abstract:** A dinuclear metal ion complex  $Zn_2(L2O)$  and its mononuclear analogue  $Zn(L1OH)$  were synthesized and studied as catalysts of the cleavage of the phosphate diester 2-hydroxypropyl-4-nitrophenyl phosphate (HPNP). X-ray crystal structure data, potentiometric titrations, and  $^1H$  NMR spectra obtained over a wide range of pH values provide strong evidence that the alcohol linker in the complex  $Zn_2(L2O)$  is ionized below pH 6.0, while the alcohol group in the complex  $Zn(L1OH)$  remains protonated even at high pH. The ionizations observed at high pH correspond to the formation of the monohydroxo complexes,  $Zn_2(L2O)(OH)$  and  $Zn(L1OH)(OH)$ , with  $pK_a$ 's of 8.0 and 9.2, respectively. The pH-rate profiles of second-order rate constants for metal-ion complex-catalyzed cleavage of HPNP are reported. These show downward curvature centered at the  $pK_a$ 's for the respective zinc-bound waters, and limiting second-order rate constants at high pH of  $k_c = 0.71 M^{-1} s^{-1}$  for  $Zn_2(L2O)$  and  $0.061 M^{-1} s^{-1}$  for  $Zn(L1OH)$ . The larger catalytic activity of  $Zn_2(L2O)$  compared with  $Zn(L1OH)$  is due to the cooperative role of the metal ions in facilitating the formation of the ionized zinc-bound water at close to neutral pH and in providing additional stabilization of the rate-limiting transition state for phosphodiester cleavage.  $Zn_2(L2O)$  complex (1 M) at pH 7.6 stabilizes the transition state for the uncatalyzed reaction by 9.3 kcal/mol. Assuming that the dissociation constant determined for a diethyl phosphate inhibitor is similar to that for substrate, then ca. 2.4 kcal/mol of these stabilizing interactions are expressed in the ground-state Michaelis complex, while the bulk of these interactions are only expressed as the reaction approaches the transition state for phosphodiester cleavage.

Two metal ions are incorporated into many enzymes that catalyze the hydrolysis of phosphate ester bonds.<sup>1</sup> Following Nature's lead dinuclear Co(III),<sup>2</sup> Cu(II),<sup>3</sup> and Zn(II)<sup>4</sup> complexes have been synthesized and shown to be better catalysts for the cleavage of RNA and RNA model compounds than their

mononuclear analogues. While there has been significant progress in this area,<sup>5–10</sup> the mechanism for the cooperative interaction of metal ions in stabilizing the transition state for phosphodiester cleavage is not well understood.

A rigorous characterization of the kinetic parameters for these mono and dinuclear catalysts is essential to any assessment of catalytic effectiveness. These parameters define the magnitude of the stabilizing interactions between substrate and catalyst in the Michaelis complex and at the transition state for conversion of this complex to product. Also, combining the kinetic parameters with other physical data for the catalyst may provide important insight into the catalytic reaction mechanism.

We report here the synthesis, X-ray crystal structures and solution properties for the dinuclear metal-ion complex  $Zn_2(L2O)$  and the mononuclear complex  $Zn(L1OH)$  [Figure 1], full pH-rate profiles of second-order rate constants for catalysis of cleavage of the phosphate diester 2-hydroxypropyl-4-nitrophenyl phosphate (HPNP), and an analysis of inhibition of this

- (1) (a) Sträter, N.; Lipscomb, W. N.; Klabunde, T.; Krebs, B. *Angew. Chem., Int. Ed. Engl.* **1996**, *35*, 2024–2055. (b) Lipscomb, W. N.; Sträter, N. *Chem. Rev.* **1996**, *96*, 2375–2433. (c) Wilcox, D. E. *Chem. Rev.* **1996**, *96*, 2435–2458.
- (2) (a) Williams, N. H.; Chin, J. *Chem. Commun.* **1996**, 131–132. (b) Williams, N. H.; Cheung, W.; Chin, J. *J. Am. Chem. Soc.* **1998**, *120*, 8079–8087.
- (3) (a) Wall, M.; Hynes, R. C.; Chin, J. *Angew. Chem., Int. Ed. Engl.* **1993**, *32*, 1633–1635. (b) Young, M. J.; Chin, J. *J. Am. Chem. Soc.* **1995**, *117*, 10577–10578. (c) Liu, S.; Hamilton, A. D. *Bioorg. Med. Chem. Lett.* **1997**, *7*, 1779–1784. (d) Molenveld, P.; Engbersen, J. F. J.; Kooijman, H.; Spek, A. L.; Reinhoudt, D. N. *J. Am. Chem. Soc.* **1998**, *120*, 6726–6737. (e) Molenveld, P.; Engbersen, J. F. J.; Reinhoudt, D. N. *J. Org. Chem.* **1999**, *64*, 6337–6341. (f) Liu, S.; Hamilton, A. D. *Chem. Commun.* **1999**, 587–588. (g) Fritsky, I. O.; Ott, R.; Pritzkow, H.; Krämer, R. *Chem. Eur. J.* **2001**, *7*, 1221–1231. (h) Gajda, T.; Jancsó, A.; Mikkola, S.; Lönnberg, H.; Sirges, H. *J. Chem. Soc., Dalton Trans.* **2002**, 1757–1763.
- (4) (a) Chapman, W. H., Jr.; Breslow, R. *J. Am. Chem. Soc.* **1995**, *117*, 5462–5469. (b) Yashiro, M.; Ishikubo, A.; Komiyama, M. *J. Chem. Soc., Chem. Commun.* **1995**, 1793–1794. (c) Matsuda, S.; Ishikubo, A.; Kuzuya, A.; Yashiro, M.; Komiyama, M. *Angew. Chem., Int. Ed.* **1998**, *37*, 3284–3286. (d) Molenveld, P.; Engbersen, J. F. J.; Reinhoudt, D. N. *Eur. J. Org. Chem.* **1999**, 3269–3275. (e) Rossi, P.; Felluga, F.; Tecilla, P.; Formaggio, F.; Crisma, M.; Toniolo, C.; Scrimin, P. *J. Am. Chem. Soc.* **1999**, *121*, 6948–6949. (f) Yamada, K.; Takahashi, Y.; Yamamura, H.; Araki, S.; Saito, K.; Kawai, M. *Chem. Commun.* **2000**, 1315–1316. (g) Gajda, T.; Krämer, R.; Jancsó, A. *Eur. J. Inorg. Chem.* **2000**, 1635–1644. (h) He, C.; Lippard, S. J. *J. Am. Chem. Soc.* **2000**, *122*, 184–185. (i) Albedyhl, S.; Schnieders, D.; Jancsó, A.; Gajda, T.; Krebs, B. *Eur. J. Inorg. Chem.* **2002**, 1400–1409.

- (5) Chin, J. *Curr. Opin. Chem. Biol.* **1997**, *1*, 514–521.
- (6) Prativel, G.; Bernadou, J.; Meunier, B. *Adv. Inorg. Chem.* **1998**, *45*, 251–312.
- (7) Krämer, R.; Gajda, T. *Perspect. Bioinorg. Chem.* **1999**, *4*, 209–240.
- (8) Williams, N. H.; Takasaki, B.; Wall, M.; Chin, J. *Acc. Chem. Res.* **1999**, *32*, 485–493.
- (9) Molenveld, P.; Engbersen, J. F. J.; Reinhoudt, D. N. *Chem. Soc. Rev.* **2000**, *29*, 75–86.
- (10) Cowan, A. J. *Curr. Opin. Chem. Biol.* **2001**, *5*, 634–642.

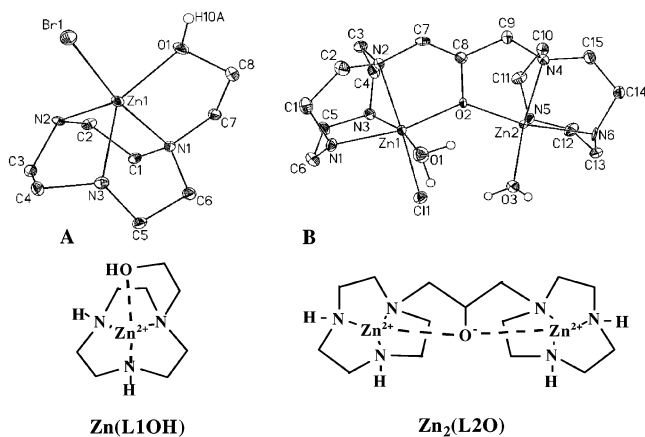


**Figure 1.** ORTEP diagrams showing the 50% probability thermal ellipsoids for all non-hydrogen atoms and schemes of the cations: (A)  $[Zn(L1OH)(Br)]^+$ . Selected bond lengths [Å]: Zn(1)–N(1) = 2.249(3), Zn(1)–N(2) = 2.096(3), Zn(1)–N(3) = 2.086(3), Zn(1)–O(1) = 2.041(2), Zn(1)–Br(1) = 2.4267(5). B)  $[Zn_2(L2O)(Cl)(H_2O)_2]^{2+}$ . Selected bond lengths [Å]: Zn(1)–N(1) = 2.133(5), Zn(1)–N(2) = 2.210(5), Zn(1)–N(3) = 2.166(5), Zn(1)–O(1) = 2.292(4), Zn(1)–O(2) = 2.014(4), Zn(1)–Cl(1) = 2.464(2), Zn(1)···Zn(2) = 3.656(2), Zn(2)–N(4) = 2.140(5), Zn(2)–N(5) = 2.110(5), Zn(2)–N(6) = 2.142(5), Zn(2)–O(2) = 1.956(4), Zn(2)–O(3) = 2.051(4).

reaction by diethyl phosphate monoanion (DEP). These data show that the stabilization of the transition state for cleavage of HPNP at pH 7.6 under conditions where the catalyzed reaction is kinetically bimolecular, 9.3 kcal/mol, is about 50% of that possible for enzymatic catalysis. A comparison of the pH-rate profiles and phosphate inhibition of the mono- and dinuclear catalysts provides interesting insight into the nature of the strong, presumably electrostatic, stabilization of the transition state for the reaction catalyzed by the dinuclear complex  $Zn_2(L2O)$ .

## Experimental Section

All reagents were reagent grade and were used without further purification, unless otherwise noted. All water was purified using a MILLI-Q system. The 1,4,7-triazacyclononane ligand,<sup>11</sup> L1OH (HBr salt),<sup>12</sup> and the barium salt of 2-hydroxypropyl-4-nitrophenyl phosphate (HPNP)<sup>13</sup> were synthesized by literature procedures. L2OH was prepared as the HCl salt by adaptation of a published procedure in which the ligand nitrogens were protected by *t*-Boc rather than tosyl groups.<sup>14</sup> The concentration of metal ion in solutions of  $Zn(NO_3)_2$  was determined by titration with EDTA using Eriochrome Black T as an indicator.<sup>15</sup> Stock solutions (10 mM) of the Zn(II) complexes of L1OH and L2OH for kinetic experiments were prepared in water by mixing  $Zn(NO_3)_2$  and L1OH·3HBr or L2OH·6HCl in 1:1.1 and 2:1.1 molar ratios, respectively, and adjusting the pH to 6.5–7.0. <sup>1</sup>H NMR spectra were recorded on a Varian Unity Inova 500 spectrometer.

**X-ray Crystallographic Analyses.** Crystalline Zn(II) complexes of L1OH and L2OH suitable for X-ray crystallography studies were prepared, respectively, as bromide and perchlorate salts as described in the Supporting Information. X-ray diffraction data were collected at 90(1) K on a Bruker SMART1000 CCD diffractometer equipped with the rotating anode (Mo K $\alpha$  radiation,  $\lambda = 0.71073$  Å). Four sets of

frames (600 frames/set) were collected, covering half of reciprocal space using  $\omega$  scans technique (0.3° frame width), with different  $\varphi$  angle. Reflection intensities were integrated using SAINTPLUS program.<sup>16</sup> The solution and refinement of the structure was performed with SHELXTL program package.<sup>17</sup> The structure was refined by full-matrix least squares against  $F^2$ .

**$[Zn(L1OH)(Br)](Br)$ .** The crystal appeared to be a racemic twin. The twin law (–1 0 0, 0 –1 0, 0 0 –1) was introduced in the refinement, with one BASF parameter<sup>17</sup> refined to 0.43(1). Non-hydrogen atoms were refined anisotropically. The positions of hydrogen atoms were found from the difference electron density Fourier synthesis. Subsequently, the hydrogen atoms were refined as riding atoms using a value of  $U_{iso}$  for the hydroxyl hydrogen that is 1.5 times larger than  $U_{eq}$  for the host oxygen, and in all other cases values of  $U_{iso}$  that are 1.2 times larger than  $U_{eq}$  for the host atom.

**$[Zn_2(L2O)(Cl)(H_2O)_2](ClO_4)_2$ .** Non-hydrogen atoms were refined anisotropically. Disorder was observed in the position of one of the perchlorate counterions, with each of two oxygen atoms lying at two positions with the occupancies obtained by isotropic structural refinement of 60/40 and 75/25. The positions of hydrogen atoms were determined by difference electron density Fourier synthesis. The hydrogen atoms were refined as riding atoms using a value of  $U_{iso}$  for the water hydrogen that is 1.5 times larger than  $U_{eq}$  for the host oxygen, and in all other cases values of  $U_{iso}$  that are 1.2 times larger than  $U_{eq}$  for the host atom. Due to the disorder in one of the counterions, Cl–O distances of the disordered ion were constrained to be 1.430(5) Å.<sup>18</sup>

**Kinetic Analyses.** The transesterification of HPNP was monitored by following the increase in absorbance at 400 nm due to the release of 4-nitrophenolate ion. The following buffers were used in these experiments: 2-(*N*-morpholino)ethanesulfonic acid (MES, pH 6–6.5), *N*-(2-hydroxyethyl)piperazine-*N'*-(2-ethanesulfonic acid) (HEPES, pH 7.1–7.8), *N*-(2-hydroxyethyl)piperazine-*N'*-(3-propanesulfonic acid) (EPPS, pH 8.0–8.4), 2-(*N*-cyclohexylamino)ethanesulfonic acid (CHES, pH 8.9–9.3) and 3-(cyclohexylamino)-1-propanesulfonic acid (CAPS, pH 10–10.5). The reactions were initiated by mixing 3–10  $\mu$ L of HPNP with 0.90 mL of solutions at 25 °C that contained catalyst and in some experiments, diethyl phosphate monoanion, and 20 mM of the appropriate buffer at  $I = 0.1$  M ( $NaNO_3$ ) to give a final HPNP concentration of 0.02 mM for reactions at pH > 6.5 or of 0.05 mM for reactions at pH 6.0 and 6.5. Pseudo-first-order rate constants  $k_{obsd}$  ( $s^{-1}$ ) for transesterification of HPNP were generally determined from the slopes of semilogarithmic plots of reaction progress against time, which were linear for at least three reaction half-times. In all cases the standard deviation for the values of  $k_{obsd}$  was <6%. In a few experiments the transesterification of HPNP was monitored for only the first 5% of reaction and the values of  $k_{obsd}$  were determined by the method of initial rates. Second-order rate constants  $k_{Zn}$  ( $M^{-1} s^{-1}$ ) for the catalyzed reactions were determined as the slope of linear plots of  $k_{obsd}$  against catalyst concentration.

## Results

$Zn(L1OH)$  and  $Zn_2(L2O)$  are used here to designate all species present at a particular pH in solution. Specific species will be indicated as needed.

**X-ray Crystal Structures.** Figure 1A shows the X-ray crystal structure of the complex cation of  $[Zn(L1OH)(Br)](Br)$  from crystals grown in water at pH 9.1. The Zn(II) ion is bound to a neutral alcohol, bromide ion, and triazamacrocycle with distorted trigonal bipyramidal geometry. Figure 1B shows the

(11) Atkins, T. J.; Richman, J. E.; Oettle, W. F. *Org. Synth.* **1978**, *58*, 86–98.  
 (12) McCue, K. P. Ph.D. Dissertation, University at Buffalo, The State University of New York, 1999.  
 (13) Brown, D. M.; Usher, D. A. *J. Chem. Soc.* **1965**, 6558–6564.  
 (14) Kimura, E.; Aoki, S.; Koike, T.; Shiro, M. *J. Am. Chem. Soc.* **1997**, *119*, 3068–3076.  
 (15) Titrimetric Analysis. *Vogel's Textbook of Quantitative Inorganic Analysis*; Bassett, J., Denney, R. C., Jeffery, G. H., Mendham, J., Eds.; John Wiley & Sons: New York, 1978.

(16) SMART and SAINTPLUS. Area detector control and integration software, Ver. 6.01. Bruker Analytical X-ray Systems: Madison, Wisconsin, 1999.  
 (17) SHELXTL. An integrated system for solving, refining and displaying crystal structures from diffraction data, Ver. 5.10; Bruker Analytical X-ray Systems: Madison, Wisconsin, 1997.  
 (18) Allen, F. H.; Kennard, O.; Watson, D. G.; Brammer, L.; Orpen, A. J.; Taylor, R. *J. Chem. Soc., Perkin Trans. II* **1987**, 1–19.

structure of  $[\text{Zn}_2(\text{L2O})(\text{Cl})(\text{H}_2\text{O})_2](\text{ClO}_4)_2$  from crystals grown in water at pH 6.0. Zn(1) in this complex is chelated to a triazamacrocycle, alkoxide and chloride ions, and a water molecule with distorted octahedral geometry, while Zn(2) is chelated to a triazamacrocycle, the alkoxide ion, and a water molecule with distorted square pyramidal geometry. The two metal ions are separated by 3.66 Å, and the electrostatic interaction between them is shielded by the ionized alkoxide bridge. In contrast the alcohol group in  $[\text{Zn}(\text{L1OH})(\text{Br})](\text{Br})$  is neutral.

**Potentiometric Titrations.** Potentiometric titration of  $\text{L2OH}\cdot 6\text{HCl}$  (1 mM) in the presence of 2 equivs of Zn(II) at 25 °C and  $I = 0.1$  M ( $\text{NaNO}_3$ ) gives two well-defined inflections (Supporting Information). The inflection at low pH marks the release of six protons from the macrocycle nitrogens and of a seventh from the linker oxygen that accompanies the binding of two Zn(II) to form  $\text{Zn}_2(\text{L2O})$ . The second inflection is centered at pH 8.0. There is no significant change in the  $^1\text{H}$  NMR chemical shift of the protons for the alcohol linker at  $\text{Zn}_2(\text{L2O})$  between pD 6.9 and 9.9 (Supporting Information). This provides strong evidence that the alcohol linker, which is ionized for crystals grown at pH 6.0 in water, remains ionized as the pD is increased from 6.9 to 9.9. We therefore propose that the ionization with  $\text{p}K_a$  of 8.0 observed for potentiometric titration of  $\text{Zn}_2(\text{L2O})$  is due to deprotonation of a coordinated water to form  $\text{Zn}_2(\text{L2O})(\text{OH})$ .

Potentiometric titration of  $\text{L1OH}\cdot 3\text{HBr}$  (1mM) in the presence of 1 equiv of Zn(II) at 25 °C and  $I = 0.1$  M ( $\text{NaNO}_3$ ) gives an inflection at low pH that marks the release of three protons upon binding of Zn(II). A second inflection centered at pH 9.2 is also observed. There is no significant change in the  $^1\text{H}$  NMR chemical shift of the protons for the alcohol pendent arm of  $\text{L1OH}$  between pD 7.9 and 10.4 (Supporting Information). This provides evidence that the alcohol group, which is protonated for crystals grown at pH 9.1, remains protonated as the pD is increased to 10.4. We therefore propose that the ionization with  $\text{p}K_a$  of 9.2 observed for potentiometric titration of  $\text{Zn}(\text{L1OH})$  is also due to deprotonation of a coordinated water to form  $\text{Zn}(\text{L1OH})(\text{OH})$ .

**Kinetic Analyses.** The transesterification of the phosphate diester HPNP catalyzed by  $\text{Zn}_2(\text{L2O})$  and by  $\text{Zn}(\text{L1OH})$  was monitored by following the increase in absorbance at 400 nm due to the release of 4-nitrophenolate.  $^{31}\text{P}$  NMR showed that the product of both catalyzed reactions was the cyclic phosphate ester. Plots of  $k_{\text{obsd}}$  against catalyst concentration are linear through  $[\text{Cat}] = 2.0$  mM for  $\text{Zn}_2(\text{L2O})$  and  $[\text{Cat}] = 4.0$  mM for  $\text{Zn}(\text{L1OH})$ .<sup>19</sup> There is no sign of downward curvature due to saturation that would result from conversion of the substrate to the Michaelis complex with catalyst. Second-order rate constants ( $k_{\text{Zn}}$ ,  $\text{M}^{-1} \text{s}^{-1}$ ) for transesterification of HPNP catalyzed by  $\text{Zn}_2(\text{L2O})$  and by  $\text{Zn}(\text{L1OH})$ , determined as the slopes of these correlations, are reported in Table 1.

$$k_{\text{Zn}} = \left( \frac{k_c K_a}{K_a + [\text{H}^+]} \right) \quad (1)$$

Figure 2 shows the plots of  $k_{\text{Zn}}$  ( $\text{M}^{-1} \text{s}^{-1}$ ) from Table 1 against pH. The solid lines were calculated from the logarithmic form

(19) The observation of clean first-order kinetics for the reaction of HPNP, and of linear plots of  $k_{\text{obsd}}$  against [catalyst] require  $K_m \gg [\text{catalyst}]$ , for [catalyst] = 0.20–2.0 mM for  $\text{Zn}(\text{L2O})$  and 0.40–4.0 mM for  $\text{Zn}(\text{L1OH})$ .

**Table 1.** Second-Order Rate Constants,  $k_{\text{Zn}}$ , for Transesterification of HPNP Catalyzed by  $\text{Zn}_2(\text{L2O})$  and  $\text{Zn}(\text{L1OH})$  at 25 °C,  $I = 0.1$  M  $\text{NaNO}_3$  and 20 mM Buffer

$\text{Zn}_2(\text{L2O})^a$		$\text{Zn}(\text{L1OH})^a$	
pH	$(k_{\text{Zn}})/10^{-2} (\text{M}^{-1} \text{s}^{-1})$	pH	$(k_{\text{Zn}})/10^{-2} (\text{M}^{-1} \text{s}^{-1})$
6.02	1.1	7.61	0.13
6.53	4.7	8.02	0.35
7.12	13	8.42	0.90
7.61	25	8.90	2.5
7.82	40	9.32	4.2
8.03	45	10.00	6.1
8.42	56	10.51	5.9
8.92	67		
9.31	68		
10.05	71		

<sup>a</sup> The ranges of catalyst concentration used in these experiments were: 0.20–2.0 mM for  $\text{Zn}_2(\text{L2O})$  and 0.50–4.0 mM for  $\text{Zn}(\text{L1OH})$ .

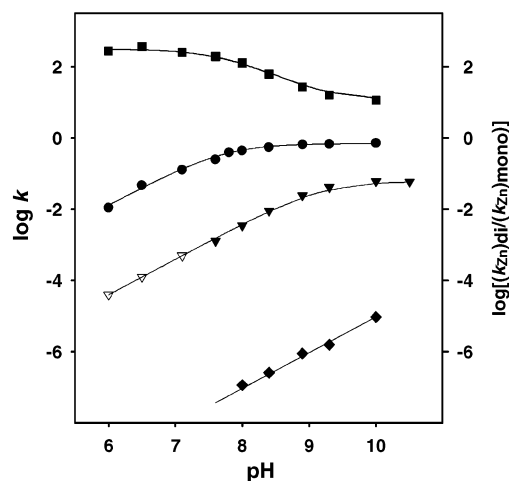


**Figure 2.** pH-rate profiles for the cleavage of HPNP: (◆,  $\text{s}^{-1}$ ) spontaneous cleavage in water [values determined by the method of initial rates]; (▼,  $\text{M}^{-1} \text{s}^{-1}$ ) cleavage catalyzed by  $\text{Zn}(\text{L1OH})$ ; (●,  $\text{M}^{-1} \text{s}^{-1}$ ), cleavage catalyzed by  $\text{Zn}_2(\text{L2O})$ ; (■), the ratio of rate constants for cleavage catalyzed by  $\text{Zn}_2(\text{L2O})$  and  $\text{Zn}(\text{L1OH})$ . The open triangles show rate constants calculated by extrapolation of the theoretical fit of data to eq 1.

#### Scheme 1



of eq 1, derived from Scheme 1, using values of  $\text{p}K_a = 7.8$  and  $k_c = 0.71 \text{ M}^{-1} \text{s}^{-1}$ ; and  $\text{p}K_a = 9.2$  and  $k_c = 0.061 \text{ M}^{-1} \text{s}^{-1}$ , respectively, for the reactions catalyzed by  $\text{Zn}_2(\text{L2O})$  and  $\text{Zn}(\text{L1OH})$ .<sup>20</sup> Figure 2 also shows the pH-rate profile for uncatalyzed transesterification of HPNP.

The stability of complexes between the mononuclear and dinuclear catalysts and diethyl phosphate monoanion (DEP), a model phosphate diester, was determined by examining DEP inhibition of catalysis of the transesterification of HPNP. Figure 3 shows a plot of normalized first-order rate constants ( $k_{\text{obsd}}/k_c$ ) for transesterification of HPNP at pH 7.6 at increasing [DEP]. Only weak inhibition is observed for the reaction catalyzed by  $\text{Zn}(\text{L1OH})$ , and these data can be fit to a simple Scheme [not shown] where HPNP and diethyl phosphate compete for binding to a single site at the catalyst. The solid line shows the nonlinear least-squares fit of the normalized data to eq 2 for competitive inhibition obtained using a value of  $K_i = 94 \text{ mM} \pm 4 \text{ mM}$  for the dissociation constant for the catalyst–inhibitor complex.

(20) The values of the  $\text{p}K_a$  for  $\text{Zn}_2(\text{L2O})$  and  $\text{Zn}(\text{L1OH})$  determined by potentiometric analysis and kinetic analysis (Figure 2) agree to within  $\pm 0.1$ .

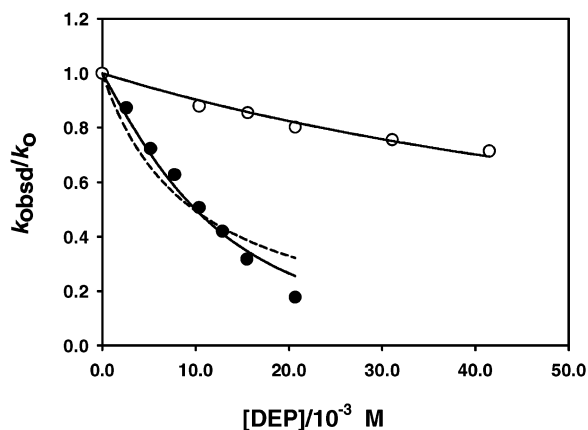
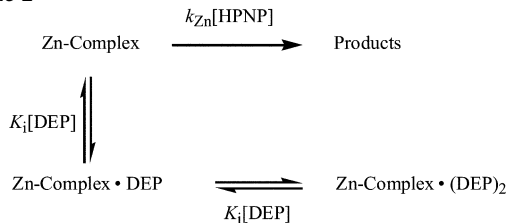


**Figure 3.** Normalized first-order rate constants for transesterification of HPNP at increasing [DEP], where  $k_o$  is the observed first-order rate constant determined for reaction in the absence of inhibitor: (●) Cleavage catalyzed by  $\text{Zn}_2(\text{L2O})$ . The dashed and solid lines show the fits of data to Schemes where the complex binds one and two molecules of inhibitor, respectively. (○) Cleavage catalyzed by  $\text{Zn}(\text{L1OH})$  using values of  $k_{\text{obsd}}$  ( $\text{s}^{-1}$ ) determined by the method of initial rates. The solid line shows the fit of data to a Scheme where the complex binds one molecule of inhibitor.

#### Scheme 2



$$\frac{k_{\text{obsd}}}{k_o} = \left( \frac{k_{\text{Zn}}[\text{Zn-Complex}]}{1 + \frac{[\text{DEP}]}{K_i}} \right) \frac{1}{k_o} \quad (2)$$

$$\frac{k_{\text{obsd}}}{k_o} = \left( \frac{k_{\text{Zn}}[\text{Zn-Complex}]}{1 + \frac{[\text{DEP}]}{K_i} + \frac{[\text{DEP}]^2}{K_i^2}} \right) \frac{1}{k_o} \quad (3)$$

DEP monoanion shows a more complex pattern of inhibition of transesterification of HPNP catalyzed by the dinuclear complex  $\text{Zn}_2(\text{L2O})$ . The dashed line in Figure 3 shows the nonlinear least-squares fit of the normalized data to eq 2, using a value of  $K_i = 10$  mM. A much better nonlinear least-squares fit of these data is obtained for Scheme 2, where the catalyst binds two molecules of DEP with equal affinity, using eq 3 with a value of  $K_i = 16 \pm 1$  mM (solid line, Figure 3).

#### Discussion

The X-ray crystal structures, potentiometric titrations, pH-rate profiles, and inhibition data for a simple phosphate diester reported here provide a complete description of the rate accelerations for catalysis of cleavage of HPNP, and an unusually detailed description of the roles of the metal ions in the Michaelis complex and transition states for these reactions.

**X-ray Crystal Structures.** The crystal structure of  $[\text{Zn}_2(\text{L2O})(\text{Cl})(\text{H}_2\text{O})_2](\text{ClO}_4)_2$  features a bridging alkoxide with the two Zn(II) ions separated by 3.66 Å. This distance is in the range (3.0–4.0 Å) observed for other related alkoxo-bridged

dinuclear Zn(II) complexes<sup>4i,21–23</sup> and for dinuclear Zn(II) cores of many metallohydrolases.<sup>1b</sup> Interestingly, the two Zn(II) ions have different coordination numbers and geometries despite the symmetry of the ligand **L2OH**, highlighting the structural flexibility of Zn(II). The crystal structure of  $[\text{Zn}(\text{L1OH})(\text{Br})-(\text{Br})]$  confirms that a neutral alcohol group is coordinated to Zn(II). The Zn–O bond distance of 2.04 Å is similar to that reported for other mononuclear Zn(II) complexes with alcohol pendent groups.<sup>24,25</sup>

**Potentiometric Titrations.** The formation of  $\text{Zn}_2(\text{L2O})$  and  $\text{Zn}(\text{L1OH})$  from  $\text{L1OH} \cdot 3\text{HBr}$  and  $\text{L2OH} \cdot 6\text{HCl}$ , respectively, was studied by potentiometric titrations. The low value of  $\text{p}K_a < 6$  observed for the alcohol linker in  $\text{Zn}_2(\text{L2O})$  is attributed to coordination of the alkoxide ion to two Zn(II) ions. Facile deprotonation of an alcohol upon binding of two Zn(II) has also been observed by Kimura<sup>21</sup> and Valtancoli<sup>22</sup> for similar dinuclear Zn(II) complexes. The relatively high  $\text{p}K_a$  of 8.0 for the water ligand in  $\text{Zn}_2(\text{L2O})(\text{H}_2\text{O})$  suggests that a terminal hydroxide complex is formed: a lower  $\text{p}K_a$  is expected for a bridging hydroxide group that interacts with both Zn(II) ions.<sup>4h,26</sup> For the mononuclear complex  $\text{Zn}(\text{L1OH})$  the alcohol remains protonated while a coordinated water is deprotonated, with a  $\text{p}K_a$  of 9.2, to form the monohydroxo complex  $\text{Zn}(\text{L1OH})(\text{OH})$ . Ionization of a zinc-bound water molecule in preference to an alcohol was also observed by Kimura for the Zn(II) complex of (1-(2-hydroxyethyl)-1,4,7,10-tetraazacyclododecane).<sup>24</sup> It is interesting that ionization of both the mononuclear and dinuclear complexes at basic pH is due to loss of a proton from a zinc-bound water, because the pH-rate profiles show that the ionization state of this water is critical for catalytic activity.

**pH-Rate Profiles.** A comparison with the less extensive kinetic analyses reported for transesterification of HPNP catalyzed by other dinuclear metal ion complexes in 100% aqueous solution places the activity of  $\text{Zn}_2(\text{L2O})$  at the upper end of these metal-ion complexes.<sup>3a,c,h,4h</sup> The pH-rate profiles of the second-order rate constants  $k_{\text{Zn}}$  for catalysis of transesterification of HPNP (Figure 2) by  $\text{Zn}_2(\text{L2O})$  and  $\text{Zn}(\text{L1OH})$  provide the following important insights into the catalytic reaction mechanism and the magnitude of the stabilization of the bound transition state.

(1) There is a downward break in the pH-rate profile for catalysis by  $\text{Zn}_2(\text{L2O})$  and by  $\text{Zn}(\text{L1OH})$  that is centered at the  $\text{p}K_a$  for deprotonation of a bound water molecule to form the monohydroxo complexes  $\text{Zn}_2(\text{L2O})(\text{OH})$  and  $\text{Zn}(\text{L1OH})(\text{OH})$ , respectively (Figure 2). These rate profiles show that the complex between HPNP and fully protonated catalysts is inactive and is converted to an active form upon loss of a proton. Kinetics provides no information about whether this proton is lost from catalyst or substrate.<sup>27</sup> However, chemical logic demands that a proton be lost from the C2-hydroxyl of HPNP

- (21) Koike, T.; Inoue, M.; Kimura, E.; Shiro, M. *J. Am. Chem. Soc.* **1996**, *118*, 3091–3099.
- (22) Bazzicalupi, C.; Bencini, A.; Berni, E.; Bianchi, A.; Fedi, V.; Fusi, V.; Giorgi, C.; Paoletti, P.; Valtancoli, B. *Inorg. Chem.* **1999**, *38*, 4115–4122.
- (23) Brudenell, S. J.; Spiccia, L.; Hockless, D. C. R.; Tiekink, E. R. T. *J. Chem. Soc., Dalton Trans.* **1999**, 1475–1481.
- (24) Koike, T.; Kajitani, S.; Nakamura, I.; Kimura, E.; Shiro, M. *J. Am. Chem. Soc.* **1995**, *117*, 1210–1219.
- (25) Li, S.; Yang, D.; Li, D.; Huang, J.; Tang, W. *New J. Chem.* **2002**, *26*, 1831–1837.
- (26) Bazzicalupi, C.; Bencini, A.; Bianchi, A.; Fusi, V.; Paoletti, P.; Piccardi, G.; Valtancoli, B. *Inorg. Chem.* **1995**, *34*, 5622–5631.
- (27) Jencks, W. P. *Catalysis in Chemistry and Enzymology*; Dover Publications: New York, 1987; Chapter 3.

on proceeding from reactant in solution to the transition state for transesterification and that the catalyst functions in some way to facilitate ionization of this hydroxyl.<sup>28</sup> There are two possible pathways for activation of HPNP by direct proton transfer from the C2-hydroxyl to the catalyst: (a) **Zn<sub>2</sub>(L2O)-(OH)** and **Zn(L1OH)(OH)** may serve as the active forms of the catalyst and act as Brønsted general base catalysts to deprotonate the C2-hydroxyl of HPNP in reactions where proton transfer to the catalyst is concerted with intramolecular addition of C2-oxygen to the phosphate diester. (b) Proton transfer from substrate to the ionized catalysts **Zn<sub>2</sub>(L2O)(OH)** or **Zn(L1OH)(OH)** may occur as a preequilibrium step to form the protonated catalysts **Zn<sub>2</sub>(L2O)(H<sub>2</sub>O)** and **Zn(L1OH)(H<sub>2</sub>O)**, respectively, and the C2-oxyanion of substrate which would then undergo nucleophilic addition to the phosphate diester. This is equivalent to the direct binding of the C2-ionized substrate to **Zn<sub>2</sub>(L2O)-(H<sub>2</sub>O)** or **Zn(L1OH)(H<sub>2</sub>O)**, followed by intramolecular addition of C2-oxygen to the phosphate diester. We assume that the high catalytic activity of these low-molecular weight catalysts is due, in part, to activation of HPNP for cleavage by direct proton transfer from the C2-hydroxyl to the catalyst. However, the pH-rate profiles shown in Figure 2 provide no information about whether this proton transfer is a discrete step in the catalytic cycle or if the putative active forms of substrate and catalyst are generated by proton-transfer reactions at free [uncomplexed] substrate and catalyst.

(2) A comparison of the second-order rate constant  $k_{Zn} = 0.25 \text{ M}^{-1} \text{ s}^{-1}$  for transesterification of HPNP catalyzed by **Zn<sub>2</sub>(L2O)** and the first-order rate constant  $k_{uncat} = 3.8 \times 10^{-8} \text{ s}^{-1}$  for the uncatalyzed reaction at pH 7.6 shows that the transition state for the catalyzed reaction is stabilized by 9.3 kcal/mol for a reaction in the presence of 1 M catalyst.

(3) The pH-rate profile (Figure 2) of the ratio of second-order rate constants for catalysis by **Zn(L1OH)** and **Zn<sub>2</sub>(L2O)** shows that the enhanced activity of the dinuclear compared to that of the mononuclear complex is due to: (a) the larger activity of the ionized dinuclear compared to mononuclear catalyst, as shown by the limiting ratio of 12 at high pH where both catalysts show maximum activity and (b) the greater ease of formation of the essential ionized zinc-bound water at **Zn<sub>2</sub>(L2O)** ( $pK_a = 7.8$ ) compared with **Zn(L1OH)** ( $pK_a = 9.2$ ), as shown by the increase in the rate constant ratio to a limiting value of 290 for reactions at low pH.

We conclude that the enhanced catalytic activity of **Zn<sub>2</sub>(L2O)** compared with **Zn(L1OH)** is due to the cooperative roles of the metal ions at the highly charged cationic core of the dinuclear catalyst in facilitating loss of a proton from the Michaelis complex between catalyst and substrate HPNP, and in providing additional stabilization of the rate-limiting transition state for the reaction of the fully active [deprotonated] Michaelis complex.

**Ground-State and Transition-State Effects.** The stabilizing interactions between these catalysts and HPNP may be expressed at the ground-state Michaelis complex and result in a tight binding affinity of the substrate for catalyst, or they may only develop on proceeding to the reaction transition states.

We have examined inhibition by diethyl phosphate monoanion of the **Zn<sub>2</sub>(L2O)**-catalyzed reaction of HPNP at pH 7.6 to obtain an estimate of the stabilization of the Michaelis complex

**Table 2.** Comparison of the Kinetic Parameters and Transition-State Stabilization for the Cleavage of HPNP Catalyzed by **Zn<sub>2</sub>(L2O)** and **Zn(L1OH)** at pH 7.6

	<b>Zn<sub>2</sub>(L2O)</b>	<b>Zn(L1OH)</b>	$\Delta\Delta G$ (kcal/mol) <sup>e</sup>
$k_{Zn}$ ( $\text{M}^{-1} \text{s}^{-1}$ ) <sup>a</sup>	0.25	0.0013	3.1
$K_i \approx K_m$ (M) <sup>b</sup>	0.016	0.094	1.0
$(k_{cat})_{obsd}$ ( $\text{s}^{-1}$ ) <sup>c</sup>	$4.1 \times 10^{-3}$	$1.2 \times 10^{-4}$	2.1
$(k_{cat})_{lim}$ ( $\text{s}^{-1}$ ) <sup>d</sup>	0.01	$5 \times 10^{-3}$	0.4

<sup>a</sup> Observed second-order rate constant for the metal-ion complex cleavage reaction at pH 7.6. <sup>b</sup> Value of  $K_i$  for competitive inhibition of the metal-ion complex cleavage reaction by diethyl phosphate at pH 7.6, which is assumed to be approximately equal to  $K_m$  for binding of HPNP. <sup>c</sup> Estimated value of  $k_{cat}$  for the metal-ion complex cleavage reaction at pH 7.6 calculated from  $k_{Zn}$  and the estimated value of  $K_m$ . <sup>d</sup> Estimated limiting value of  $k_{cat}$  at high pH calculated with the assumption that the pH-rate profiles that govern  $k_{Zn}$  (Figure 2) and  $(k_{cat})_{obsd}$  are the same. <sup>e</sup> The difference, calculated from the ratio of rate or equilibrium constants on the left, in the relative stabilization of the Michaelis complex or transition state by interaction of HPNP with **Zn<sub>2</sub>(L2O)** and **Zn(L1OH)**.

by interaction with a simple phosphate monoanion. Figure 3 shows the decrease in the observed first-order rate constant for **Zn<sub>2</sub>(L2O)**-catalyzed hydrolysis of HPNP at increasing concentrations of diethyl phosphate. These data show a poor fit to eq 2 derived for a simple Scheme (not shown) in which HPNP and diethyl phosphate monoanion compete for binding to a single site at the catalyst. However, they show a good fit to eq 3, derived for Scheme 2, in which two molecules of diethyl phosphate monoanion bind sequentially to **Zn<sub>2</sub>(L2O)** with equal dissociation constants of  $K_i = 16 \text{ mM}$ . The simple interpretation of these data is that each metal ion in the dinuclear catalyst coordinates to a single diethyl phosphate. By analogy, this dinuclear complex may coordinate to two molecules of substrate, or to one molecule of substrate and one molecule of inhibitor. If the latter termolecular complex forms, then it must be catalytically inactive, since our data show a good fit to Scheme 2 in which binding of a single diethyl phosphate monoanion renders the catalyst inactive.

By comparison, there is relatively little inhibition of **Zn(L1OH)**-catalyzed hydrolysis of HPNP by diethyl phosphate monoanion (Figure 3): these data were fit to eq 2 derived for a Scheme (not shown) in which the catalyst binds only a single molecule of diethyl phosphate monoanion with  $K_i = 94 \text{ mM}$ . Together the data for **Zn<sub>2</sub>(L2O)** and **Zn(L1OH)** provide evidence that each Zn(II) ion of these complexes binds to a single diethyl phosphate monoanion. The 6-fold tighter binding affinity of diethyl phosphate monoanion to **Zn<sub>2</sub>(L2O)** compared with **Zn(L1OH)** reflects the stronger electrostatic stabilization at the more highly cationic dinuclear complex.

The observed second-order rate constants  $k_{Zn}$  for catalysis of transesterification at pH 7.6 (Table 2) are equivalent to  $k_{cat}/K_m$  for enzyme catalysts. Table 2 also lists values of  $K_m \approx K_i$  for inhibition of cleavage by diethyl phosphate monoanion determined at pH 7.6 and estimates of  $(k_{cat})_{obsd}$  calculated from the values for  $k_{Zn}$  and  $K_m$ . The maximum value of  $k_{cat}$  at high pH was then estimated by assuming that the pH-rate profiles that govern the values of  $k_{Zn}$  ( $\text{M}^{-1} \text{s}^{-1}$ ) and  $(k_{cat})_{obsd}$  are the same.

Table 2 shows that the barrier for formation of transition state from free catalyst and substrate ( $k_{Zn} = k_{cat}/K_m$ ) at pH 7.6 is 3.1 kcal/mol lower for the reaction catalyzed by the dinuclear complex compared to that by the mononuclear complex. This difference can be divided into a 1.0 kcal/mol preferential stabilization of the Michaelis complex at **Zn<sub>2</sub>(L2O)** ( $K_m$  effect) and a further 2.1 kcal/mol stabilization of the transition state for cleavage of

(28) Wolfenden, R.; Snider, M. J. *Acc. Chem. Res.* **2001**, *34*, 938–945.

bound substrate ( $k_{cat}$  effect). Most of the difference in the barriers to ( $k_{cat}$ )<sub>obsd</sub> is due to the larger fraction of catalytically active Michaelis complexes for  $Zn_2(L2O)$  compared that for to  $Zn(L1OH)$  at pH 7.6. Only a small 0.4 kcal/mol difference is estimated in the stabilities of the transition states for reaction at high pH where these catalysts show maximum value of ( $k_{cat}$ )<sub>lim</sub> (Table 2).

We conclude that the difference in the catalytic power of  $Zn_2(L2O)$  and  $Zn(L1OH)$  at pH 7.6 is due mainly to the greater stabilization of the Michaelis complex and the larger relative concentration of the catalytically active form of  $Zn_2(L2O)$ . Our data also provide evidence that the values of ( $k_{cat}$ )<sub>lim</sub> for turnover of these two catalysts at high pH are similar.

**Origin of the Catalytic Power of  $Zn_2(L2O)$ .** The transition state for the transesterification of HPNP catalyzed by  $Zn_2(L2O)$  at pH 7.6 is stabilized by 9.3 kcal/mol. Values of  $k_{cat}/K_m \approx (10^6 - 10^7) M^{-1} s^{-1}$  are typically observed for enzymatic catalysis of phosphodiester cleavage,<sup>29</sup> so that the low-molecular weight catalyst  $Zn_2(L2O)$  has achieved about one-half of the possible ca. 20 kcal/mol stabilization possible for highly efficient protein catalysts.

The 9.3 kcal/mol transition-state stabilization may result either from hydrophobic interactions between nonpolar parts of the substrate HPNP and  $Zn_2(L2O)$ , or from stabilizing electrostatic interactions between the anionic substrate and cationic catalyst. Since our catalysts are small and lack any obvious shape complementarity with substrate, it is probable that transition-state stabilization arises mainly from electrostatic interactions. The activity of this catalyst toward cleavage of RNA and RNA analogues might easily be enhanced by increasing these binding interactions through tethering  $Zn_2(L2O)$  to recognition agents.

The estimated dissociation constant of  $K_i \approx K_m = 16$  mM for catalysis of the reaction of HPNP by  $Zn_2(L2O)$  at pH 7.6 shows that only about 2.4 of the 9.3 kcal/mol transition state stabilization is due to ground-state interactions with the phosphate monoanion. The remaining 7 kcal/mol of stabilization may represent stabilizing electrostatic interactions between the cationic catalyst and negative charge at the C2-oxygen, or interactions that only develop on proceeding from the Michaelis complex to the transition state for cleavage of HPNP. This discrimination between binding of substrate and transition state that is characteristic of enzyme catalysis is particularly difficult to model in small molecule catalysts. If the interactions between  $Zn_2(L2O)$  and bound substrate in the transition state are primarily electrostatic, then the selectivity in transition-state binding must reflect, in some sense, a redistribution of negative charge at the substrate on proceeding to the transition state that moves negative charge toward the cationic metal ions of the catalyst. One possibility is that the Zn(II) ion coordinates to the phosphate monoanion of HPNP and that this coordination strengthens as the formal negative charge at this functional group increases from  $-1$  at the phosphate monoanion of substrate to  $-2$  at the oxyphosphorane-like transition state for the transesterification reaction.

**Acknowledgment.** We thank the National Science Foundation (CHE 9986332) for support of this work.

**Supporting Information Available:** Potentiometric pH titration data, <sup>1</sup>H NMR titration spectra and kinetic rate constants for the uncatalyzed transesterification of HPNP (PDF). X-ray crystallographic files (CIF). This material is available free of charge via the Internet at <http://pubs.acs.org>.

(29) Raines, R. T. *Chem. Rev.* **1998**, *98*, 1045–1065.